AGU100 ADVANCING EARTH AND SPACE SCIENCE

Geophysical Research Letters

RESEARCH LETTER
10.1029/2018GL081052

Key Points:
- The Geostationary Lightning Mapper is a new instrument and the first of its kind to observe lightning from geostationary orbit
- The GLM is revolutionary in its ability to continuously monitor total lightning distributions throughout its near-hemispheric field of view
- GLM flashes are less common over the oceans, but the oceanic flashes are larger, brighter, and last longer than flashes over land

Correspondence to:
S. D. Rudlosky,
scott.rudlosky@noaa.gov

Citation:
Rudlosky, S. D., Goodman, S. J., Virts, K. S., & Bruning, E. C. (2018). Initial geostationary lightning mapper observations. *Geophysical Research Letters*, *45*. https://doi.org/10.1029/2018GL081052

Received 6 SEP 2018
Accepted 15 NOV 2018
Accepted article online 21 NOV 2018

Initial Geostationary Lightning Mapper Observations

Scott D. Rudlosky[1], Steven J. Goodman[2], Katrina S. Virts[3], and Eric C. Bruning[4]

[1]National Oceanic and Atmospheric Administration, Center for Satellite Applications and Research, College Park, MD, USA, [2]Thunderbolt Global Analytics, Huntsville, AL, USA, [3]NASA/Marshall Space Flight Center, Huntsville, AL, USA, [4]Department of Geosciences, Texas Tech University, Lubbock, TX, USA

Abstract The Geostationary Lightning Mapper (GLM) continuously observes lightning throughout a near-hemispheric field of view, capturing spatiotemporal variability on unprecedented scales. This study documents GLM lightning distributions during the initial 9 months in the operational Geostationary Operational Environmental Satellite-East position (December 2017 to August 2018). Spatial maps, summary statistics, and time series illustrate seasonal, regional, and diurnal lightning patterns. Lightning activity shifts from south to north during the study period with most lightning over land (83%). The average GLM flash extends over a 454-km^2 area, lasts 301 ms, produces 262 fJ of optical energy, and consists of 16.4 (42.2) groups (events). On average, GLM flashes over the oceans are larger (570 km^2), of longer duration (345 ms), and brighter (420 fJ) than flashes over land (431 km^2, 293 ms, and 230 fJ). The baseline values and early insights reported herein aim to guide the early development and application of GLM observations.

Plain Language Summary The Geostationary Lightning Mapper (GLM) is the first sensor of its kind, and this technological advancement now allows continuous operational monitoring of total lightning on time and space scales never before available. The GLM has entered into a golden age of lightning observations, which will spur more rapid progress toward synthesis of lightning observations with other meteorological data sets and forecasting tools. This study documents the first 9 months of GLM operations to introduce this new lightning data source and demonstrate the value of this new technology. Within the first 9 months, the GLM captured similar spatial patterns of lightning occurrence to many previous studies covering much longer periods of time. The present study shows that GLM flashes were less common over the oceans, but that the oceanic flashes were larger, brighter, and lasted longer than flashes over land. The ability to continuously sample lightning distributions throughout the GLM field of view allows detailed analysis of the diurnal cycle (e.g., Lake Maracaibo). The GLM presents exciting new possibilities, with countless new applications anticipated over the coming decades.

1. Introduction

The first Geostationary Lightning Mapper (GLM) launched on 19 November 2016 aboard the initial Geostationary Operational Environmental Satellite (GOES) R-series spacecraft. The GOES-R became GOES-16 upon reaching geostationary orbit on 29 November 2016, continuing the 40+-year GOES mission. GOES-16 spent nearly a year in the checkout position (89.5°W) before moving to its operational position (75.2°W) and becoming the new GOES-East on 18 December 2017.

The GOES-East GLM is the first of four instruments in the GOES-R series (R, S, T, and U) that will provide lightning mapping over most of the Western Hemisphere through 2036. The GLM mission objectives are to provide early indication, tracking, and monitoring of storm intensification and severe weather; enable increased tornado warning lead time; and provide data continuity for long-term climatology studies (Goodman et al., 2013). The GLM performance requirements include greater than 70% flash detection efficiency, flash false alarm rate less than 5%, and location accuracy within a half a pixel.

The GLM provides continuous total lightning measurements over the Americas and adjacent oceans with coverage to 54°N/S. It detects total lightning, both intracloud and cloud-to-ground, although it does not natively distinguish between these two lightning types. The GLM was designed to detect >70% of all flashes when averaged over 24 hr, with better performance anticipated at night (~90%) than during the day (~70%). The GLM is a new instrument that continues to undergo extended calibration and validation.

The GLM is the first step in an international space-based observing constellation for continuous total lightning measurements on a global scale. Both the Meteosat Third Generation (Stuhlmann et al., 2005) and

Chinese Fengyun-4 (Yang et al., 2017) geostationary satellites will host optical lightning imagers. The GLM builds on a legacy of optical lightning observations from low Earth orbit including the Lightning Imaging Sensor (LIS) on the Tropical Rainfall Measuring Mission (TRMM) satellite (Albrecht et al., 2016). The GLM results from decades of work toward detecting lightning from geostationary orbit.

Lightning is now designated as a Global Climate Observing System Essential Climate Variable needed to understand and predict changes in climate (Aich et al., 2018). The lightning Essential Climate Variable is envisioned as an integrated global data set composed of well-characterized ground- and space-based lightning observations. The GLM will extend measurements of lightning variability and change for the next two decades, ensuring establishment of a 30+-year optical lightning data set.

This study introduces the GLM by documenting the lightning distributions during the initial 9 months in the GOES-East position (December 2017 to August 2018). Spatial plots and summary statistics illustrate the seasonal and regional lightning patterns, and diurnal cycle analyses demonstrate the value of routine GLM monitoring. Many operational applications will benefit from the GLM observations, so it is important to clearly convey the attributes of this new information. These baseline values and initial insights aim to guide the early development and application of the GLM observations.

2. Data

The GOES-R Product Definition and User's Guide details the GLM instrument, including the functional characteristics, content, and format of the GLM data (GOES-R, 2017). The instrument specifications referenced below draw from this document. The GOES-R Data Book (GOES-R Series Data Book, 2018) provides additional information on the GLM instrument design.

The GLM is a Charge-Coupled Device imager with a set of optical filters to detect lightning in a narrow ~1-nm spectral band centered on 777.4 nm (i.e., near infrared). The GLM consists of a single telescope with a variable pitch focal plane detector array of 1,372 by 1,300 pixels. The array is divided into 56 subarrays for fast transient event processing by 56 Real-Time Event Processors (RTEPs). Each subarray is independently tuned to optimize the dynamic range and sensitivity, which vary based on the background scene. The variable pitch reduces the spatial growth of GLM pixel footprints away from nadir, so the pixel size only varies from ~8 km at nadir to ~14 km at the limb.

The instrument relies on the spacecraft position and pointing information along with a coastline identification and navigation procedure to convert the focal plane x, y to latitude and longitude coordinates. The GLM Level 2 product navigates the observations to an estimated cloud top based on an assumed lightning ellipsoid height that varies from 6 km at the poles to 16 km at the equator. Scientists are investigating refinements to the cloud top height assumption to improve navigation and reduce spatial offsets that can occur when correlating the lightning to observations from other satellites, weather radar, and ground-based lightning networks. The first related modification to the ground system software adjusted the equatorial height assumption from 16 to 14 km beginning 15 October 2018.

The GOES ground system produces Level 2 data files that contain information on GLM events, groups, and flashes (GOES-R Algorithm Working Group and GOES-R Series Program, 2018; GOES-R Series Data Book, 2018; Goodman et al., 2013). The GLM tracks the average background brightness value at each pixel. Each new 2-ms sample is compared to the background values to detect sudden changes in brightness, triggering event detections when the new sample exceeds a selectable detection threshold. A suite of filters in the ground-processing software remove nonlightning events leaving only the 2-ms events most likely to be lightning. The Lightning Cluster Filter Algorithm is the final processing step that combines events into groups and groups into flashes. GLM groups represent one or more simultaneous GLM events observed in adjacent pixels, and GLM flashes consist of one or more sequential groups separated by less than 330 ms and 16.5 km (Mach et al., 2007).

3. Methods

The first 9 months of GLM observations from the operational GOES-East position were subset into 3 climatic seasons (December, January, and February—DJF; March, April, and May—MAM; and June, July, and August—

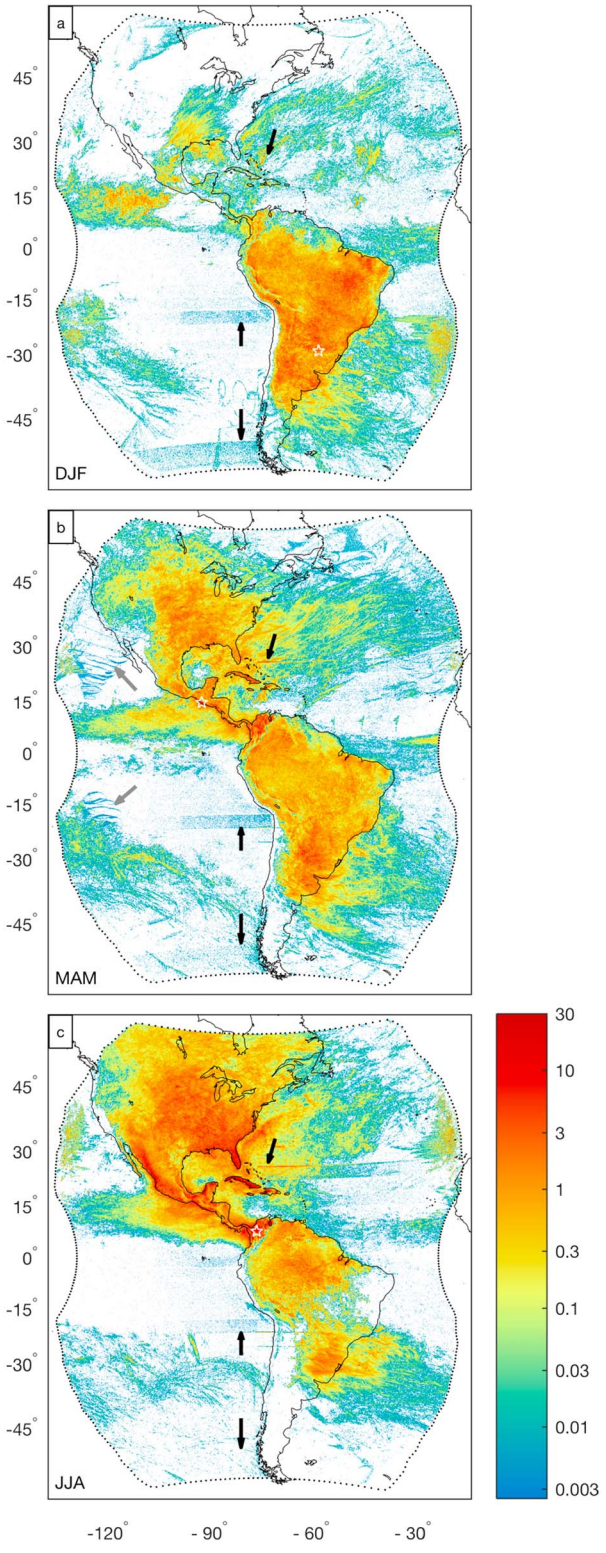

Figure 1. Seasonal GLM lightning flash density (flashes km^{-2} mon^{-1}) during (a) December 2017 to February 2018, (b) March–May 2018, and (c) June–August 2018. The white stars on each panel indicate the lightning maximum during each season. Arrows indicate data quality artifacts (see section 4.2).
GLM = Geostationary Lightning Mapper; DJF = December, January, and February; MAM = March, April, and May; JJA = June, July, and August.

JJA) to illustrate the seasonal variability. Spatial flash density maps are plotted at 0.1° resolution with units of flashes per square kilometer per month.

Tuning of the ground system algorithms and RTEP thresholds continued during the 9-month study period (additional improvements are planned). This study characterizes the data as originally produced and archived, with the exception of quality control steps that help mitigate known sources of false events. Each GLM L2 data file includes a *flash_quality_flag* and a *group_quality_flag*, for which 0 indicates good quality, while larger integers indicate degraded flashes or groups. This study removes flashes with *flash_quality_flag≠0* and groups with *group_quality_flag≠0*. Groups also are removed if the parent flash has *flash_quality_flag≠0*, and events are removed if the parent group (grandparent flash) has *group_quality_flag≠0* (*flash_quality_flag≠0*). These steps help but do not completely eliminate the effects of Sun glint or solar intrusion during eclipse season (see section 4.2).

Additional GLM quantities plotted at 0.1° resolution show more attribute variability. This study illustrates the average GLM flash area, flash duration, and flash energy and also characterizes group area, group energy, event energy, number of groups per flash, number of events per flash, and number of events per group. The flash and group properties are accumulated using their centroid locations (i.e., no consideration of the event footprints/spatial extent of groups and flashes). Studies on finer spatial and temporal scales are encouraged to move beyond the centroid locations to leverage GLM information on the full spatial extent of flashes and groups. The table provides mean, median, and 90th and 99th percentile values for each GLM quantity. For computational efficiency, the percentile values are calculated individually for each day, with the table reporting the medians of the daily 50th, 90th, and 99th percentile values.

4. Results

4.1. Seasonal, Regional, and Diurnal Variability

In just 9 months the GLM captured spatial and temporal lightning patterns at a resolution equivalent to the observations accumulated over 16 years described by previous studies (e.g., Albrecht et al., 2016; Beirle et al., 2014; Cecil et al., 2014; Christian et al., 2003). The GLM observed 237,100,495 flashes during the 9-month study period, comprising over 3.8 billion groups and nearly 10 billion events. Overall, 83% (17%) of the GLM flashes occurred over land (ocean), with most lightning over land during all 3 seasons. The greatest lightning activity shifted from south to north as the seasons progressed. During DJF, 86% of the GLM flashes occurred in the Southern Hemisphere (SH). The Northern Hemisphere (NH) exhibited 84% of the GLM flashes during JJA, with a more even spread during MAM (NH: 55% versus SH: 45%).

Figure 1 illustrates the seasonal shift in lightning occurrence from the SH to the NH during the study period. Most lightning occurred over South America during local summer (DJF; Figure 1a). The relative maxima correspond to known topographical influences and meteorological regimes. One relative maxima occurred near the Argentina/Brazil

Table 1
The Mean, Median, and 90th and 99th Percentile Values of GLM Flash Area, Flash Duration, Flash Energy, Number of Groups per Flash, Number of Events per Flash, Number of Events per Group, Group Area, Group Energy, and Event Energy

Overall	Mean	Median	90th	99th	Land	Ocean
Flash area (km^2)	454	291	965	2,570	431	570
Flash duration (ms)	301	240	626	1,170	293	345
Flash energy (fJ)	261	90	658	2,390	230	420
Groups per flash (count)	16.4	10.0	40.0	83.0	15.4	21.3
Events per flash (count)	42.2	22.0	106.0	267.0	39.3	57.0
Events per group (count)	2.6	2.0	5.0	14.0	2.5	2.8
Group area (km^2)	180	135	350	1,010	175	196
Group energy (fJ)	16.2	6.1	33.6	153.0	15.1	20.0
Event energy (fJ)	6.2	3.1	12.2	48.8	6.0	7.1

Note. Values report the medians of the daily 50th, 90th, and 99th percentile values. Mean values also are reported over the land and oceans. GLM = Geostationary Lightning Mapper.

border (local maximum 10.6 fl km^{-2} mon^{-1}; 29.15°S, 57.05°W), while additional maxima appeared where the trade winds encountered the coastal highlands of northeastern Brazil and over the foothills of the Andes Mountains. In the NH, relative maxima appeared over the east central Pacific and within a region of comparable flash densities over the southern United States and the Gulf of Mexico. Individual storm tracks can greatly influence the short-term cool season distributions.

Lightning activity was more evenly distributed between the SH and NH during MAM (Figure 1b). The maximum MAM flash densities occurred over the foothills of the Sierra Madre range in southwestern Guatemala (15.6 fl km^{-2} mon^{-1}; 14.55°N, 91.65°W) and over northern Colombia and Lake Maracaibo in Venezuela, which Albrecht et al. (2016) identified as the Earth's top lightning hot spot. Other relative maxima coincided with the climatological location of severe storms in the south central United States and southeastern Brazil.

The maximum GLM flash density during JJA occurred over northwestern Colombia (27.3 fl km^{-2} mon^{-1}; 7.55°N, 75.45°W; Figure 1c). Relative maxima also occurred over Central America, Cuba, and the southeastern United States, and enhanced flash densities appeared in association with the Gulf Stream current off the U.S. East Coast. During NH summer, frequent lightning also extended into Canada, with some locations observing 1–3 fl km^{-2} mon^{-1}.

The GLM maps the full spatial extent of the cloud illuminated by lightning, and the rapidly updating optical lightning observations provide helpful insights into the flash and storm structure (e.g., Peterson, Deierling, et al., 2017; Peterson & Liu, 2013; Peterson, Rudlosky, & Deierling et al., 2017; Peterson et al., 2018). Table 1 reveals that the average GLM flash extended over an area of 454 km^2, had a mean duration of 301 ms, produced 261 fJ of optical energy at the sensor aperture, and consisted of 16.4 (42.2) groups (events). The average GLM group extended 180 km^2, produced 16 fJ, and contained 2.6 events. Note that the average areal extent of TRMM LIS flashes (313 km^2; Beirle et al., 2014) was ~69% the area of the average GLM flash (454 km^2; Table 1). Larger GLM pixels likely contribute to the larger average GLM flash area. Small cloud top optical sources (i.e., few square kilometers in size) can illuminate up to four LIS or GLM pixels depending on the source brightness and location. Flashes that LIS maps as 16–64 km^2 could map to 64–256 km^2 using the GLM.

Although lightning occurs less frequently over the oceans (Figure 1), oceanic lightning flashes are brighter on average than lightning flashes over land (Figure 2). Table 1 reveals that GLM flashes over the oceans were larger (570 km^2), of longer duration (345 ms), and brighter (420 fJ) than flashes over land (431 km^2, 293 ms, and 230 fJ). This supports previous studies that documented a tendency for stronger, more horizontally extensive lightning flashes over the oceans using both ground-based radio (Cooray et al., 2014; Hutchins et al., 2013; Said et al., 2013) and space-based optical (Beirle et al., 2014; Peterson, Rudlosky, & Deierling, 2017; Rudlosky & Shea, 2013) lightning observations. Additional research is required to better understand the tendency for stronger flashes over the oceans.

Figure 2 suggests that certain land regions also are more susceptible to larger and longer flashes. For example, large, long duration flashes were relatively common in portions of North and South America where mesoscale convective systems frequently produce horizontally extensive stratiform flashes. In contrast, flashes and groups over the Andes and Rocky Mountains were generally smaller and of shorter duration. This contrast was particularly apparent between the central Andes and the foothills and lowlands to the east.

An innovative aspect of the GLM is the ability to continuously detect lightning at every location within its near-hemispheric field of view. This allows total lightning distributions to be tracked throughout entire storm lifecycles (not shown) and the diurnal cycle at any location (Figure 3). Intermittency in the diurnal cycle, which varies daily, provides important meteorological insights. This is especially true in regions with complex interactions between large-scale flow, local topography, and mesoscale meteorology. Due to a low-altitude, low-

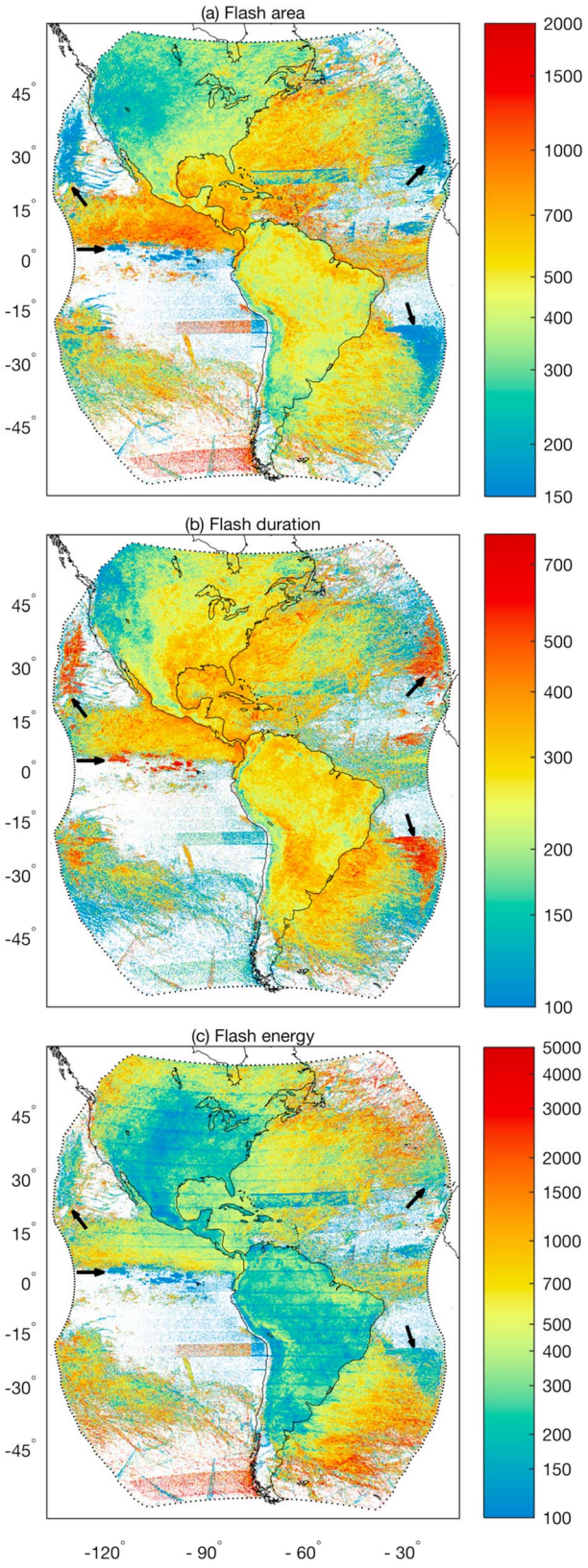

Figure 2. Mean Geostationary Lightning Mapper observed (a) flash area (km^2), (b) flash duration (ms), and (c) flash energy (fJ). Arrows indicate data quality artifacts (see section 4.2).

inclination orbit that precessed through the local diurnal cycle (Simpson et al., 1988), the TRMM LIS required 49 days to observe most places at least once during each local hour (Albrecht et al., 2016). Thus, LIS could require up to 35 years to sample the diurnal cycle for the equivalent of the 257 days (~9 months) studied here. Comparison of Figure 3 to Figure 3 in Albrecht et al. (2016) shows that the GLM observations resulted in smoother diurnal curves, with reduced statistical uncertainty—as expected for twice as much view time.

The diurnal cycles for Lake Maracaibo (land versus lake) and the central United States demonstrate some important GLM insights (Figure 3). Over the land areas surrounding Lake Maracaibo, daytime heating of the elevated terrain produced a late-afternoon lightning frequency maximum (~18:00 local time; Figure 3b). The land-based diurnal trends were very similar to the diurnal cycle in the central United States (Figure 3h). The greatest flash densities in the Lake Maracaibo domain occurred over the lake during a nocturnal peak at ~2:00 local time (Figure 3e). Albrecht et al. (2016) described the unique features that contribute to the development of deep convection over Lake Maracaibo an average of 297 days per year with a nighttime maximum. Routine GLM monitoring now provides the potential to rapidly advance our knowledge of the lightning activity in this interesting region.

Figure 3 indicates secondary lightning frequency spikes near solar noon over both Lake Maracaibo and the surrounding land (absent in the central United States). The GLM flash area and duration follow similar diurnal trends in each domain (Figures 3c, 3f, and 3i). In general, larger flashes lasted longer, with a nocturnal maximum in both flash area and duration. A notable exception appeared near solar noon over both the lake and surrounding land. The secondary lightning frequency spikes resulted from small ($<$200 km^2) longer duration ($>$350 ms) flashes, indicating artifacts from Sun glint and blooming (section 4.2). Although the glint effect is greatest over the lake, its appearance over the surrounding land areas illustrates the blooming or cascading of false events away from their source location.

Deviations from the mean values documented herein provide useful context when interpreting and applying the GLM data. The observed physical variability fits expectations from earlier TRMM LIS investigations as well as studies using ground-based lightning observations, demonstrating the feasibility of GLM use for global scale weather and climate applications on interannual time scales. Careful quality control is required, as evidenced by the data quality artifacts appearing in the initial data, which will continue to improve in time with tuning of the instrument and algorithms.

4.2. Artifacts

Figure 1b reveals some data quality artifacts that are less apparent during the other seasons. An example occurred off the west coast of Mexico, with the same swirl pattern also apparent farther south (gray arrows; Figure 1b). The direct source of these patterns remains under investigation but the patterns likely related to known sources of false events. Somewhat more subtle are a few remaining subarray boundaries that require additional calibration and tuning (black arrows; Figure 1). These regions appeared as rectangles demarcated by enhanced flash density along their edge occurring east of the Bahamas and off the west coast of Chile (one north and one south). Some of these data quality artifacts were less apparent in

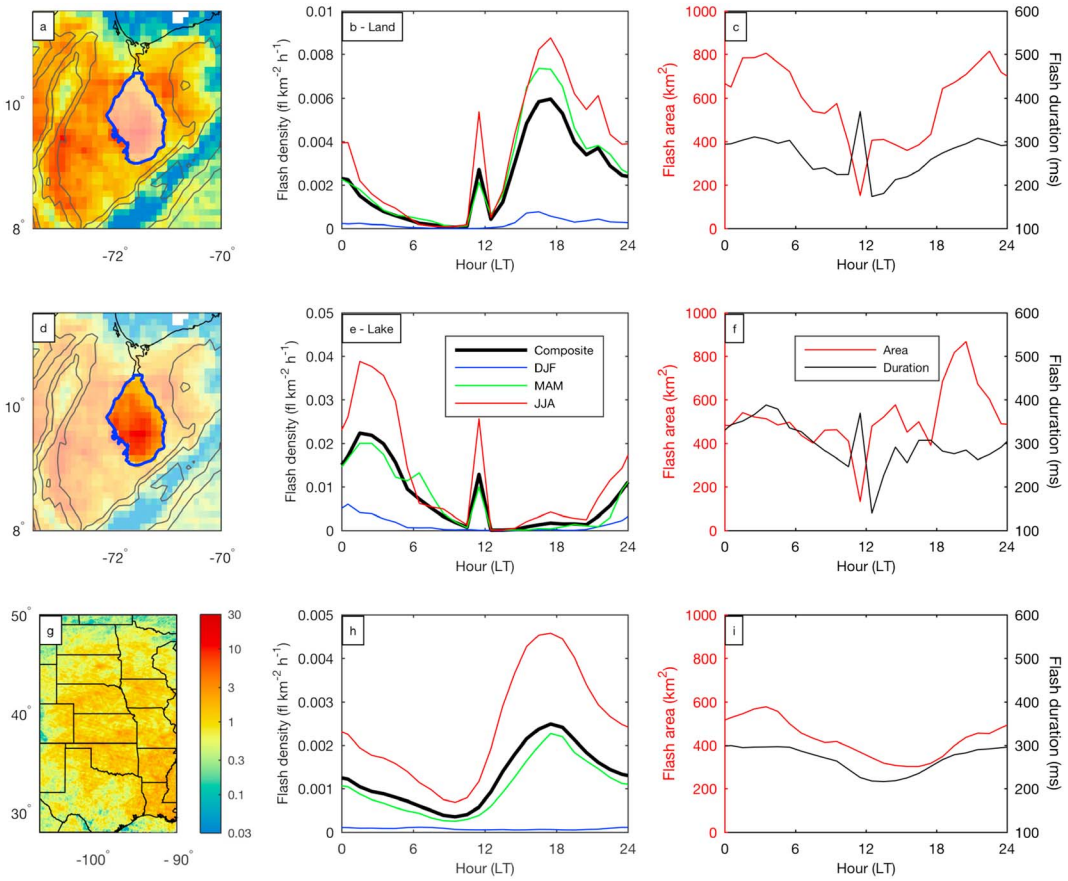

Figure 3. Illustration depicting the diurnal lightning cycle over the land areas surrounding Lake Maracaibo (a–c), Lake Maracaibo (d–f), and the central United States (g–i). The left column illustrates the domains, composite 9-month flash densities, and topography (300, 1000, and 3000 m elevation contours, panels a and d). The middle column shows the mean flash density for each season as well as the composite (note the different scale magnitudes), and the right column shows the composite mean flash area (red) and duration (black). LT = local time; DJF = December, January, and February; MAM = March, April, and May; JJA = June, July, and August.

Figure 1c due in part to one source of false events (i.e., platform disturbances during daylight hours) becoming less common and impactful during JJA.

The data quality artifacts in the flash density maps are more apparent in plots of the other GLM characteristics (black arrows; Figure 2). In addition to investigating long time series of lightning properties, these additional GLM parameters can help diagnose data quality in real time. One somewhat common source of false events is river, lake, and ocean glint that occur when specific Sun angles combine with relatively calm bodies of water. Regions susceptible to glint exhibited flashes with small areas (Figure 2a) and long durations (Figure 2b). The most apparent examples occurred along the equator in the Pacific Ocean and over the eastern most portions of the field of view (one north and one south).

Solar intrusion during the eclipse seasons provides an example of false events that only can be mitigated (i.e., cannot be completely removed). During certain days and times, direct solar illumination nearly reaches the GLM focal plane, resulting in false detection artifacts that quickly bloom into massive numbers of false events. A blooming filter has been developed to improve data quality and is awaiting implementation in the GOES ground system. The blooming filter quenches the rapid growth of artifacts associated with both Sun glint and eclipse effects.

False GLM events also arise when the GLM platform stability is disturbed during daylight hours. This jitter results in many false events along cloud edges. Most commonly, these false events relate to brief momentum adjust maneuvers that are required to maintain proper spacecraft location and orientation. Calibration scans for other instruments on the satellite also produce false events. Attempts are made to schedule these calibration scans at night to minimize their impact. Adjustments to the RTEP thresholds during July 2018 marginally reduced the GLM sensitivity in part to lessen the platform stability-related false events.

False events occur at subarray boundaries when improperly tuned RTEPs combine with bright clouds that are nearly stationary. This issue produced the most apparent artifacts in Figure 2, evident as large rectangular regions east of the Bahamas and off the west coast of Chile. When bright clouds persist over certain RTEP boundaries, the threshold to noise ratio drops, sensitivity increases, and false events ensue. A fix for this has been developed and is awaiting implementation in the GOES ground system.

5. Future Work

Technological advancement now allows continuous operational monitoring of total lightning on time and space scales never before available. The GLM has entered into a golden age of lightning observations, which are presently near the beginning of an expansion begun by other remote sensing platforms decades prior. While lightning specialists and curious operational users have eagerly applied the initial data, focused efforts will be required to ensure data fidelity and the development of the most useful operational products. The GLM will supplement the foundational data sets (i.e., radar, visible, infrared, and microwave imagery), filling gaps where needed, and increasing the information available to operational users. The continuous availability of spatially extensive total lightning data will spur more rapid progress toward synthesis of these observations with other meteorological data sets and forecasting tools.

The GLM data quality continually improves as known issues are patched and new issues are identified and addressed. The most impactful remaining data quality issues stem from Sun glint and solar intrusion. These phenomena produce blooming artifacts that result in false detections that quickly cascade into large numbers of false events. These event spikes can slow or stop the processing chain resulting in missing and/or empty files. A blooming filter that quenches the rapid growth of artifacts associated with both Sun glint and eclipse effects has been developed and is awaiting implementation in the GOES ground system.

The GLM presents exciting new possibilities, with countless new applications likely over the coming decades. An unforeseen application showed that the GLM also detects bolides (or fireballs) as they enter the Earth atmosphere (Jenniskens et al., 2018). These observations motivated the authors to envision GLM use for automated bolide detection. Gridded GLM products were developed and integrated into the National Weather Service operations to promote application by forecasters. The initial gridded GLM products (flash extent density, average flash area, and total optical energy) provide the National Weather Service forecasters with a new perspective on lightning activity, and the forecasters will in turn help drive GLM innovation. The GOES-West GLM greatly expands coverage and provides a large overlapping region from which to further exploit the GLM capabilities.

Acknowledgments
Funding for this project was provided by the NOAA/NESDIS via STAR/GOES-R and the Cooperative Institute for Climate and Satellites–Maryland (CICS-MD). The NASA Postdoctoral Program supported the tremendous contributions of coauthor Katrina Virts. The authors thank the countless individuals and teams that have supported GLM development, integration, science, and application. The authors acknowledge significant contributions to this effort from William Koshak, Peter Armstrong, Samantha Edgington, and Clem Tillier. We also thank the entire Lightning and Atmospheric Electricity Group at NASA's Marshall Space Flight Center for their support, especially Hugh Christian, Rich Blakeslee, Monte Bateman, Doug Mach, and Dennis Buechler. All GLM data are available via the National Oceanic and Atmospheric Administration (NOAA) Comprehensive Large Array-data Stewardship System (CLASS). The contents of this paper are solely the opinions of the authors and do not constitute a statement of policy, decision, or position on behalf of NOAA or the U.S. government.

References

Aich, V., Holzworth, R. H., Goodman, S. J., Kuleshov, Y., Price, C., & Williams, E. R. (2018). Lightning: A new essential climate variable. *Eos*, *99*. https://doi.org/10.1029/2018EO104583

Albrecht, R., Goodman, S., Buechler, D., Blakeslee, R., & Christian, H. (2016). Where are the lightning hotspots on Earth? *Bulletin of the American Meteorological Society*, *97*(11), 2051–2068. https://doi.org/10.1175/BAMS-D-14-00193.1

Beirle, S., Koshak, W., Blakeslee, R., & Wagner, T. (2014). Global patterns of lightning properties derived by OTD and LIS. *Natural Hazards and Earth System Sciences*, *14*(10), 2715–2726. https://doi.org/10.5194/nhess-14-2715-2014

Cecil, D. J., Buechler, D. E., & Blakeslee, R. J. (2014). Gridded lightning climatology from TRMM-LIS and OTD: Dataset description. *Atmospheric Research*, *135-136*, 404–414. https://doi.org/10.1016/j.atmosres.2012.06.028

Christian, H. J., Blakeslee, R. J., Boccippio, D. J., Boeck, W. L., Buechler, D. E., Driscoll, K. T., et al. (2003). Global frequency and distribution of lightning as observed from space by the optical transient detector. *Journal of Geophysical Research*, *108*(D1), 4005. https://doi.org/10.1029/2002JD002347

Cooray, V., Jayaratne, R., & Cummins, K. L. (2014). On the peak amplitude of lightning return stroke currents striking the sea. *Atmospheric Research*, *149*, 372–376. https://doi.org/10.1016/j.atmosres.2013.07.012

GOES-R algorithm working group and GOES-R series program (2017). Product definition and user's guide. Volume 3: Level 1b Products, 29 November 2017 DCN 7035538, Revision F.1. Retrieved from https://www.goes-r.gov/users/docs/PUG-L1b-vol3.pdf

GOES-R algorithm working group and GOES-R series program (2018). NOAA GOES-R series geostationary lightning mapper (GLM) level 2 lightning detection: Events, groups, and flashes. December 2017 – August 2018. NOAA National Centers for Environmental Information. https://doi.org/10.7289/V5KH0KK6

GOES-R Series Data Book (2018). NASA publication NP-2018-1-155-GSFC, September 2018. Retrieved from https://www.goes-r.gov/downloads/resources/documents/GOES-RSeriesDataBook.pdf

Goodman, S. J., Blakeslee, R. J., Koshak, W. J., Mach, D., Bailey, J., Buechler, D., et al. (2013). The GOES-R Geostationary Lightning Mapper (GLM). *Atmospheric Research*, *125-126*, 34–49. https://doi.org/10.1016/j.atmosres.2013.01.006

Hutchins, M. L., Holzworth, R. H., Virts, K. S., Wallace, J. M., & Heckman, S. (2013). Radiated VLF energy differences of land and oceanic lightning. *Geophysical Research Letters*, *40*, 2390–2394. https://doi.org/10.1002/grl.50406

Jenniskens, P., Albers, J., Tillier, C. E., Edgington, S. F., Longenbaugh, R. S., Goodman, S. J., et al. (2018). Detection of meteoroid impacts by the Geostationary Lightning Mapper on the GOES-16 satellite. *Meteoritics and Planetary Science*. https://doi.org/10.1111/maps.13137

Mach, D., Christian, H., Blakeslee, R., Boccippio, D., Goodman, S., & Boeck, W. (2007). Performance assessment of the optical transient detector and lightning imaging sensor. Part II: Clustering algorithm. *Journal of Geophysical Research*, *112*, D09210. https://doi.org/10.1029/2006JD007787

Peterson, M., Deierling, W., Liu, C., Mach, D., & Kalb, C. (2017). The properties of optical lightning flashes and the clouds they illuminate. *Journal of Geophysical Research: Atmospheres*, *122*, 423–442. https://doi.org/10.1002/2016JD025312

Peterson, M., Rudlosky, S., & Deierling, W. (2017). The evolution and structure of extreme optical lightning flashes. *Journal of Geophysical Research: Atmospheres*, *122*, 13,370–13,386. https://doi.org/10.1002/2017JD026855

Peterson, M., Rudlosky, S., & Deierling, W. (2018). Mapping the lateral development of lightning flashes from orbit. *Journal of Geophysical Research: Atmospheres*, *123*, 9674–9687. https://doi.org/10.1029/2018JD028583

Peterson, M. J., & Liu, C. (2013). Characteristics of lightning flashes with exceptional illuminated areas, durations, and optical powers and surrounding storm properties in the tropics and inner subtropics. *Journal of Geophysical Research: Atmospheres*, *118*, 11,727–11,740. https://doi.org/10.1002/jgrd.50715

Rudlosky, S. D., & Shea, D. T. (2013). Evaluating WWLLN performance relative to TRMM/LIS. *Geophysical Research Letters*, *40*, 2344–2348. https://doi.org/10.1002/grl.50428

Said, R. K., Cohen, M. B., & Inan, U. S. (2013). Highly intense lightning over the oceans: Estimated peak currents from global GLD360 observations. *Journal of Geophysical Research: Atmospheres*, *118*, 6905–6915. https://doi.org/10.1002/jgrd.50508

Simpson, J., Adler, R. F., & North, G. R. (1988). A proposed tropical rainfall measuring mission (TRMM) satellite. *Bulletin of the American Meteorological Society*, *69*(3), 278–295. https://doi.org/10.1175/1520=0477(1988)069<0278:APTRMM>2.0.CO:2

Stuhlmann, R., Rodriguez, A., Tjemkes, S., Grandell, J., Arriaga, A., Bézy, J.-L., et al. (2005). Plans for EUMETSAT's third generation Meteosat geostationary satellite programme. *Advances in Space Research*, *36*(5), 975–981. https://doi.org/10.1016/j.asr.2005.03.091

Yang, J., Zhang, Z., Wei, C., Lu, F., & Guo, Q. (2017). Introducing the new generation of Chinese geostationary weather satellites, Fengyun-4. *Bulletin of the American Meteorological Society*, *98*(8), 1637–1658. https://doi.org/10.1175/BAMS-D-16-0065.1